VEGF binding to NRP1 is essential for VEGF stimulation of endothelial cell migration, complex formation between NRP1 and VEGFR2, and signaling via FAK Tyr407 phosphorylation

Birger Herzog[a,b], Caroline Pellet-Many[a], Gary Britton[a], Basil Hartzoulakis[c], and Ian C. Zachary[a]
[a]BHF Laboratories and [b]Ark Therapeutics, Department of Medicine, University College London, London WC1E 6JJ, UK; [c]Xention Limited, Cambridge CB22 3EG, UK

ABSTRACT In endothelial cells, neuropilin-1 (NRP1) binds vascular endothelial growth factor (VEGF)-A and is thought to act as a coreceptor for kinase insert domain-containing receptor (KDR) by associating with KDR and enhancing VEGF signaling. Here we report mutations in the NRP1 b1 domain (Y297A and D320A), which result in complete loss of VEGF binding. Overexpression of Y297A and D320A NRP1 in human umbilical vein endothelial cells reduced high-affinity VEGF binding and migration toward a VEGF gradient, and markedly inhibited VEGF-induced angiogenesis in a coculture cell model. The Y297A NRP1 mutant also disrupted complexation between NRP1 and KDR and decreased VEGF-dependent phosphorylation of focal adhesion kinase at Tyr407, but had little effect on other signaling pathways. Y297A NRP1, however, heterodimerized with wild-type NRP1 and NRP2 indicating that nonbinding NRP1 mutants can act in a dominant-negative manner through formation of NRP1 dimers with reduced binding affinity for VEGF. These findings indicate that VEGF binding to NRP1 has specific effects on endothelial cell signaling and is important for endothelial cell migration and angiogenesis mediated via complex formation between NRP1 and KDR and increased signaling to focal adhesions. Identification of key residues essential for VEGF binding and biological functions provides the basis for a rational design of antagonists of VEGF binding to NRP1.

INTRODUCTION

Neuropilins-1 and -2 (NRP1 and NRP2) are transmembrane glycoproteins with large extracellular regions containing two CUB (homology with complement binding factors C1s/C1r, sea urchin epidermal

growth factor [uEGF] and Bone Morphogenetic Protein 1 [BMP1]) homology domains (a1, a2), two coagulation factor V/VIII homology domains (b1, b2), and a MAM (homology with meprin, A5 antigen, and receptor tyrosine protein phosphatase m) domain (Pellet-Many et al., 2008). In addition, they have a transmembrane domain and a short intracellular domain with no clearly defined signaling function (Fujisawa and Kitsukawa, 1998; Rossignol et al., 2000). The importance of NRP1 for vascular and neuronal development has been established by the generation of knockout mice, which are embryonic lethal with severe defects in the nervous system and vasculature (Kitsukawa et al., 1997; Kawasaki et al., 1999). Distinct sites in NRP1 bind semaphorins and vascular endothelial growth factor (VEGF) family members to mediate the role of these ligands in neurons and endothelial cells, respectively (He and Tessier-Lavigne, 1997; Kolodkin et al., 1997; Soker et al., 1998; Gu et al., 2002). The major VEGF binding site is located in the b1 domain with some contribution of the b2 domain, whereas the a1/a2 together with the b1/b2 domains are critical for recognition of Sema3A (Gu et al., 2002).

VEGF or VEGF-A is a specific mitogen for vascular endothelial cells which stimulates vasculogenesis and angiogenesis (Holmes

and Zachary, 2005). VEGF acts through the tyrosine kinase receptors, VEGFR1 and VEGFR2 (kinase insert domain-containing receptor; KDR). In particular, KDR is crucial in mediating VEGF signaling in endothelial cells by activating several different signaling cascades with different physiological functions including survival, proliferation, migration, vascular permeability, tubulogenesis, NO and prostanoid biosynthesis, and gene expression (Gille et al., 2001). VEGF binding to KDR activates phosphatidylinositol 3-kinase and Akt/protein kinase B, a major pathway responsible for cell survival (Gerber et al., 1998; Thakker et al., 1999). In addition, VEGF is a strong activator of phospholipase Cγ, which in turn mediates activation of Extracellular signal-regulated kinase-1 and -2 (ERK1 and ERK2), protein kinase C, and protein kinase D pathways. This activation results in diverse biological responses including increased gene expression, mitogenesis, cell migration, and prostacyclin production (Gliki et al., 2001; Takahashi et al., 2001; Evans et al., 2008). Another important mediator of VEGF signaling in endothelial cells is the Src/focal adhesion kinase (FAK) pathway, which plays an important role in cell motility and actin cytoskeleton organization (Abedi and Zachary, 1997; Abu-Ghazaleh et al., 2001). Whereas KDR is crucial for all these VEGF effects in endothelial cells, NRP1 is particularly important for cell motility and chemotactic migration but has little effect on cell division (Pan et al., 2007).

NRP1 lacks any known enzymatic activity and is thought to function in endothelial cells by enhancing VEGF binding to KDR and downstream signaling events (Soker et al., 2002). VEGF-A$_{165}$ promotes the formation of a complex of NRP1 and KDR in endothelial cells, which is thought to be important for optimal VEGF signaling and function (Soker et al., 2002). In addition, the cytosolic domain of NRP1 is required for the interaction of NRP1 and KDR (Prahst et al., 2008). This domain of NRP1 also interacts with GIPC/Synectin, which is implicated in endothelial cell migration and angiogenesis (Cai and Reed, 1999; Gao et al., 2000; Chittenden et al., 2006; Wang et al., 2006).

While there is compelling evidence for an essential role of NRP1 in angiogenesis, the precise contribution of VEGF binding to NRP1 in angiogenic or endothelial functions of NRP1 remains unclear. Furthermore, some evidence suggests that NRP1 may act independently of VEGF and KDR in stimulating cell migration and adhesion (Wang et al., 2003; Murga et al., 2005). The objective of this study was to elucidate the role of VEGF binding to NRP1 in endothelial cell function by mutational analysis of residues in the putative VEGF binding pocket within the b1 domain essential for VEGF binding. In this report we describe a mutant form of NRP1 (Y297A NRP1), which cannot bind VEGF (Jarvis et al., 2010). Overexpression of this NRP1 mutant in endothelial cells reduces complex formation between endogenous NRP1 and KDR and impairs migration of these cells toward a VEGF gradient and angiogenesis in a coculture model. Y297A NRP1 also selectively decreased phosphorylation of FAK at Y407 in endothelial cells. These results show the importance of VEGF binding to NRP1 in cell migration, and signaling linked to the regulation of actin cytoskeletal dynamics and formation of focal adhesions.

RESULTS
Identification of NRP1 b1 domain residues essential for VEGF-A$_{165}$ binding
Computational analysis of the b1 domain based on the crystal structure of NRP1 (Lee et al., 2003) revealed a putative ligand-binding pocket, which includes the amino acid residues Tyr-297 and Asp-320 (Figure 1A). These residues are evolutionarily conserved between species and are also identical in NRP2, as shown for Tyr-297 in

Figure 1B. Point mutations were introduced to evaluate the importance of these and other residues for VEGF-A$_{165}$ binding. Full-length NRP1 expression plasmids were generated in which Tyr-297 or Asp-320 had been replaced by alanine. Wild-type (WT) and mutant versions of NRP1 expression constructs were transfected into COS7 cells, which express little endogenous NRP1. Both mutants and WT NRP1 were expressed to a similar level as judged by Western blot and flow cytometry, and immunofluorescence staining indicated a similar subcellular localization to the plasma membrane (Figure 1, C–E). Next we tested the ability of the NRP1 mutants to bind biotinylated VEGF-A$_{165}$ (bt-VEGF-A$_{165}$) when expressed in COS7 cells. As shown in Figure 1F, cells expressing WT NRP1 showed increasing specific VEGF-A$_{165}$ binding over a range of VEGF-A$_{165}$ concentrations. In contrast, the Y297A point mutation showed no specific VEGF-A$_{165}$ binding at any bt-VEGF-A$_{165}$ concentrations tested, consistent with our previous results (Jarvis et al., 2010). Next we compared the effect of the Y297A mutation with other mutations. Similar to Y297A, D320A also abrogated VEGF-A$_{165}$ binding (Figure 1G). Effects of mutations of other residues comprising the VEGF-A$_{165}$ binding pocket on binding were also examined (Figures 1A and 2C).

Heparin increases VEGF-A$_{165}$ binding to NRP1 and promotes receptor dimerization of isolated proteins (Vander Kooi et al., 2007). We therefore asked if heparin would rescue the loss of VEGF-A$_{165}$ binding to Y297A NRP1 and other NRP1 VEGF binding mutants. COS7 cells were transfected with WT and mutant forms of NRP1, and VEGF binding was measured in the presence and absence of heparin. Heparin increased the binding of VEGF-A$_{165}$ to WT NRP1 but had no effect on VEGF-A$_{165}$ binding to the W301A, D320A, D320A, and Y353A mutants (Figure 2, A–C). Heparin, however, was able to enhance VEGF binding to T316A, T349A, K351A, and W411A mutants, all of which displayed markedly reduced binding in the absence of heparin (Figure 2C).

The NRP1 b1 domain is also essential for Sema3A binding (Gu et al., 2002). It was therefore important to examine the effect of the Y297A mutation on the binding of Sema3A. Measurement of Sema3A binding to WT and Y297A NRP1 expressed in COS7 showed that Sema3A binding increased with increasing levels of NRP1 expression, but revealed no difference between these two forms of NRP1 in their relative ability to bind Sema3A (Figure 2D).

NRP1 mutants unable to bind VEGF-A$_{165}$ inhibit binding to WT NRP1 and NRP2
Next we investigated the effect of the Y297A mutation on the ability of WT NRP1 to bind VEGF-A$_{165}$. Cotransfection of WT and different amounts of mutant expression plasmid resulted in increasing inhibition of high-affinity bt-VEGF-A$_{165}$ binding correlating with increasing levels of Y297A NRP1 expression, indicating a dominant-negative effect of the VEGF-binding mutant on bt-VEGF-A$_{165}$ binding in COS7 cells (unpublished results). We next examined whether Y297A NRP1 expression could similarly inhibit VEGF binding to endogenous NRP1 in human umbilical vein endothelial cells (HUVECs). In addition, because many endothelial cells, including HUVECs, coexpress NRP1 and NRP2, and both are known to bind VEGF-A$_{165}$, we also examined whether non-VEGF-binding NRP1 mutants affected VEGF-A$_{165}$ binding to NRP2. Due to the low sensitivity of bt-VEGF-A$_{165}$ binding, however, subsequent binding studies used ^{125}I-VEGF-A$_{165}$ (Jia et al., 2006).

^{125}I-VEGF-A$_{165}$ binding was observed in COS7 cells expressing either NRP1 or NRP2 (Figure 3A), although determination of binding at different ^{125}I-VEGF-A$_{165}$ concentrations indicated that binding to NRP2 was significantly lower in affinity compared with NRP1,
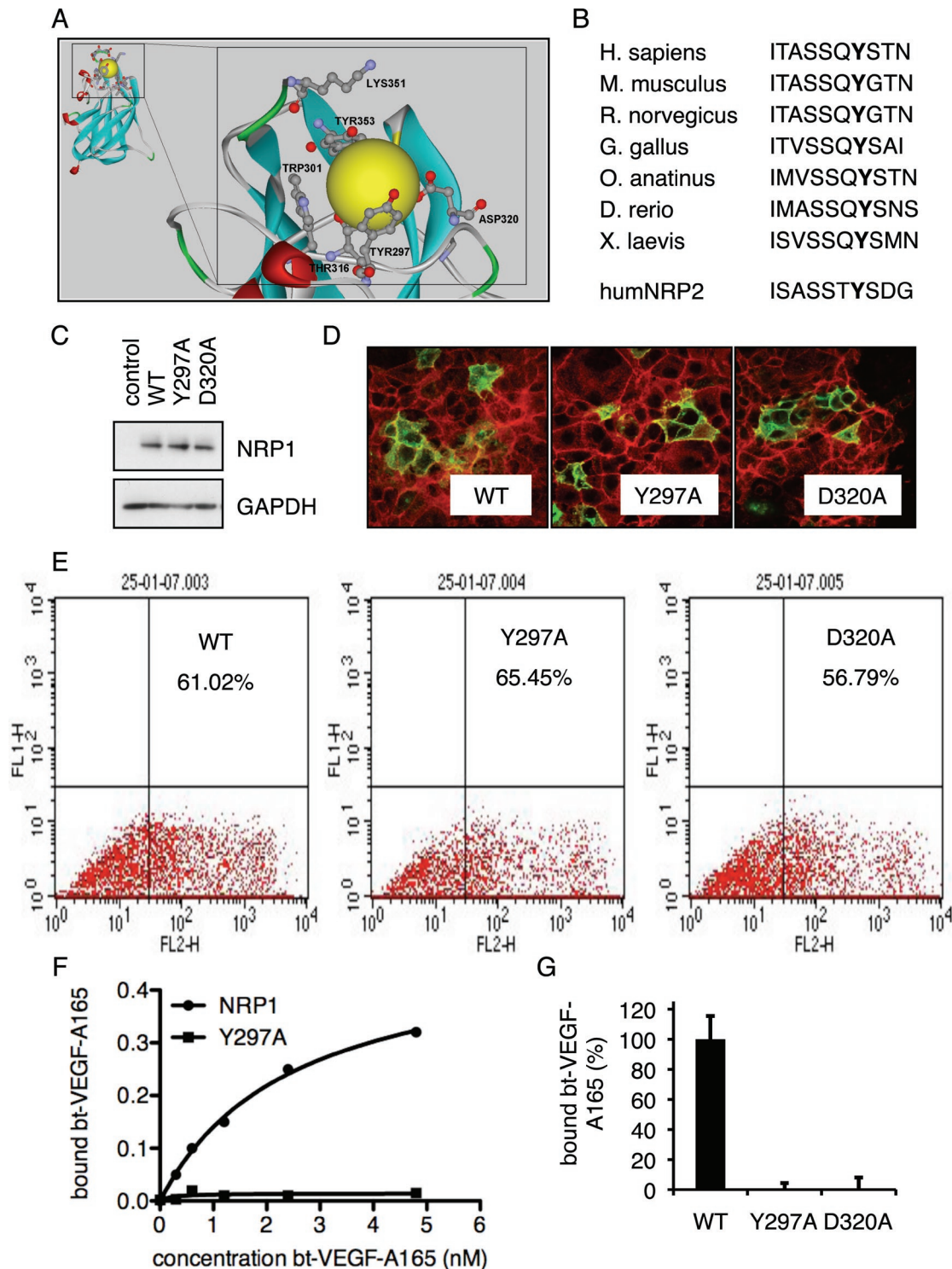
FIGURE 1: NRP1 b1 domain residues required for VEGF-A$_{165}$ binding. (A) A structural model of the VEGF binding pocket (yellow sphere) in the b1 domain of human NRP1 was generated computationally from the known b1 domain structure. Amino acids predicted to be critical for VEGF-A$_{165}$ binding are labeled. (B) The NRP1 sequence of amino acids 291–300 from different species and human NRP2 were aligned. The Tyr-297 residue is shown in bold. (C) COS7 cells were transfected with empty expression vector (control), WT NRP1 (WT), or mutant NRP1 (Y297A, D320A) expression plasmids. Western blots for NRP1 and GAPDH were performed using whole-cell extracts 48 h after transfection. (D) Immunofluorescence staining of COS7 cells expressing WT and mutant NRP1 constructs, as indicated, with antibody to NRP1 (green). (E) Flow cytometric analysis of NRP1-expressing cells was performed in COS7 cells transfected with WT, Y297A, or D320A NRP1 expression plasmids as indicated. (F) COS7 cells were infected with adenoviruses expressing WT or Y297A NRP1. Binding assays for bt-VEGF-A$_{165}$ were performed with indicated amounts of VEGF as shown 48 h after infection. (G) COS7 cells were transfected with expression plasmids encoding WT, Y297A, or D320A NRP1 as indicated. Total specific binding of bt-VEGF-A$_{165}$ was measured 48 h after transfection. Data represent means ± SD of values obtained from four to six independent experiments.
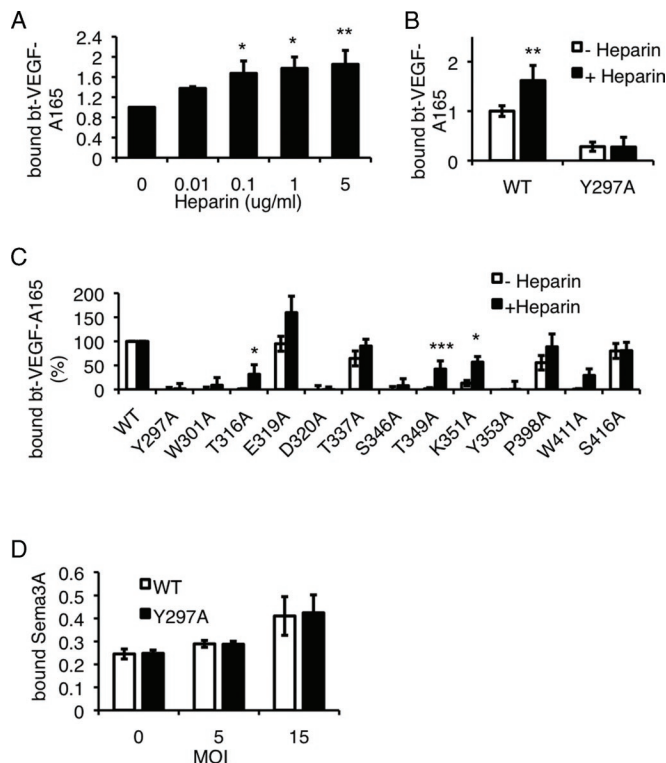
FIGURE 2: Effect of heparin on VEGF-A$_{165}$ binding to WT NRP1 and b1 domain mutants. (A) VEGF-A$_{165}$ binding assay to WT NRP1 expressing COS7 cells in the presence of increasing amounts of heparin. Data are expressed as mean fold changes ± SD in binding from three independent experiments; *p < 0.05 and **p < 0.01 vs. no heparin. (B) VEGF-A$_{165}$ binding in the absence or presence of 1 μg/ml heparin to WT and Y297A NRP1; **p < 0.01 vs. no heparin. (C) VEGF-A$_{165}$ binding in the absence or presence of 1 μg/ml heparin to WT NRP1 and NRP1 mutants, as indicated. Data are expressed as mean fold changes ± SD from three independent experiments; *p < 0.05 and ***p < 0.001 vs. WT + heparin. (D) Binding assay for Sema3A in COS7 infected with WT or Y297A NRP1 expressing adenoviruses at the indicated MOI. Data represent mean fold changes ± SD from three independent experiments.

FIGURE 3: Overexpression of Y297A NRP1 reduces VEGF-A$_{165}$ binding. (A) Binding assay of ^{125}I-VEGF-A$_{165}$ in COS7 cells transfected with fixed amounts of either WT NRP1 or WT NRP2, and increasing amounts of Y297A NRP1 expression plasmids. Numbers below the bars are ratios of Y297A to WT plasmids. Data represent mean specific binding ± SD from three independent experiments. (B) HUVECs were transfected with control siRNA (NC) and siRNAs targeted to NRP1, NRP2, or KDR. Cell lysates were immunoblotted 48 h later with the antibodies indicated. (C) HUVECs were transfected with control siRNA (NC) and siRNAs targeted to NRP1, NRP2, or KDR, and, 48 h after transfection, ^{125}I-VEGF-A$_{165}$ binding was determined in the presence or absence of a 100-fold excess unlabeled VEGF-A$_{165}$. The data shown are values for specific binding expressed as means ± SD from three independent experiments; *p < 0.05 and **p < 0.01 vs. NC. (D) HUVECs were infected with adenoviruses expressing GFP, WT NRP1, Y297A, or D320A NRP1 at different MOIs as indicated. After 72 h, ^{125}I-VEGF-A$_{165}$ binding was determined in the presence or absence of a 100-fold excess unlabeled VEGF-A$_{165}$. The data shown are values for specific binding expressed as means ± SD from three independent experiments; *p < 0.05, **p < 0.01, and ***p < 0.001 vs. no virus.

with K_d values of 8 and 0.3 nM for NRP2 and NRP1, respectively (unpublished data), consistent with previously reported K_d values of 5.2 and 0.5 nM for NRP2 and NRP1 (Geretti et al. 2007). Transfection with increasing amounts of plasmid cDNA encoding Y297A NRP1 strongly inhibited ^{125}I-VEGF-A$_{165}$ binding in COS7 cells coexpressing WT NRP1 with >80% inhibition at the highest Y297A NRP1/WT NRP1 ratio, and similarly reduced ^{125}I-VEGF-A$_{165}$ binding in COS7 cells coexpressing WT NRP2 plasmid with a maximum 90% inhibition (Figure 3A). To assess the contributions of different VEGF receptors to high-affinity ^{125}I-VEGF-A$_{165}$ binding to endothelial cells, ^{125}I-VEGF-A$_{165}$ binding was determined in HUVECs after knockdown of NRP1, NRP2, and KDR using targeted siRNAs (Figure 3B). As shown in Figure 3C, knockdown of NRP1, NRP2, and KDR significantly reduced total specific ^{125}I-VEGF-A$_{165}$ binding by ~30, 25, and 30%, respectively. We next addressed whether Y297A NRP1 could exert a dominant-negative effect on VEGF-A$_{165}$ binding to endogenously expressed NRPs in HUVECs. To achieve a high efficiency of transduction, HUVECs were infected with adenoviruses expressing control protein (AdGFP), WT NRP1 (AdWT NRP1), Y297A NRP1 (AdY297A NRP1), or D320A NRP1 (AdD320A NRP1). Expression of AdWT NRP1 enhanced ^{125}I-VEGF-A$_{165}$ binding above the level in uninfected or in AdGFP-infected
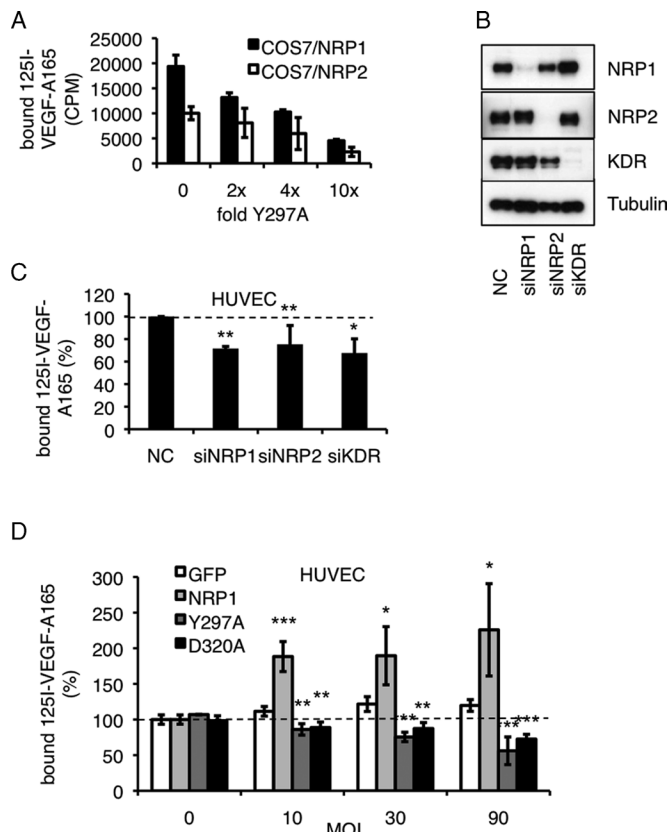
cells, but increasing multiplicity of infection (MOI) using AdWT NRP1 produced no further augmentation of binding. In contrast, AdY297A NRP1 or AdD320A NRP1 decreased ^{125}I-VEGF-A$_{165}$ binding, the degree of inhibition increasing with increasing MOI, reaching ~45 and 27% inhibition at the highest MOI tested for AdY297A NRP1 and AdD320A NRP1, respectively (Figure 3D). Because HUVECs also express NRP2, KDR, and VEGFR1/Flt1, the ^{125}I-VEGF-A$_{165}$ binding to HUVECs uninhibited by even the highest mutant NRP1 MOI is likely to reflect ^{125}I-VEGF-A$_{165}$ binding to other VEGF-A receptors.

Our findings taken together indicate that the dominant-negative effects of non-VEGF-binding NRP1 b1 domain mutants on high-affinity binding of VEGF-A$_{165}$ can be mediated via effects on both

NRP1 and NRP2, but also suggest that these mutants do not have a general inhibitory effect on ^{125}I-VEGF-A$_{165}$ binding to its other receptors when overexpressed in endothelial cells.

VEGF-A$_{165}$ binding to NRP1 is required for complex formation between NRP1 and KDR

It was next examined whether the Y297A VEGF-binding mutant was able to perturb NRP1 complexation with KDR following treatment with VEGF-A$_{165}$ (Soker *et al.*, 2002). To address this question, HUVECs were infected with adenovirus expressing V5-tagged WT NRP1 or V5-Y297A NRP1, and coimmunoprecipitations were performed using anti-V5 as the immunoprecipitating antibody followed by Western blots for KDR and for KDR phosphorylated at Y1175. VEGF-A$_{165}$ promoted complex formation between KDR and NRP1 in cells overexpressing V5-WT NRP1 as indicated by the detection of KDR and KDR phosphorylation at Y1175 in V5-WT NRP1 immunoprecipitates (Figure 4, A and B). In contrast, VEGF-induced NRP1/KDR complex formation was strongly inhibited in cells expressing the binding-deficient V5-Y297A NRP1 mutant even though immunoprecipitation of V5-Y297A NRP1 was similar to that for V5-WT NRP1 (Figure 4, A and B).

A mechanism through which the Y297A NRP1 mutant could exert a dominant-negative effect on VEGF responses is the formation of heterodimers with WT NRP1 and NRP2. Such mutant/WT heterodimers would have a reduced capacity to bind VEGF-A$_{165}$, and this in turn would be predicted to impair biological functions and signaling dependent on VEGF-A$_{165}$ binding to NRP1 or on NRP2. To determine whether Y297A NRP1 could heterodimerize with WT NRP1, YFP-tagged Y297A NRP1 was coexpressed in COS7 cells with V5-tagged NRP1, and immunoprecipitates were prepared using anti-V5 antibody and then blotted with antibody to green fluorescent protein (GFP)/yellow fluorescent protein (YFP). As shown in Figure 4C, YFP-Y297A NRP1 was specifically coimmunoprecipitated with V5-NRP1, whereas no coimmunoprecipitation was observed when untagged NRP1 was coexpressed with YFP-Y297A NRP1 or vice versa. Similarly, anti-YFP blots of V5 immunoprecipitates prepared from COS7 cells coexpressing V5-Y297A NRP1 and YFP-NRP2 demonstrated strong coimmunoprecipitation of mutant NRP1 with NRP2 (Figure 4C). We also found that WT NRP1 and NRP2 were able to heterodimerize by coimmunoprecipitation of V5-NRP1 with YFP-NRP2 (unpublished results).

VEGF-A$_{165}$ binding to NRP1 and NRP2 is important for migration of endothelial cells

We next investigated the role of VEGF-A$_{165}$ binding to NRP1 in the migration of HUVECs. Knockdown of NRP1 or NRP2 expression using siRNAs markedly reduced VEGF-induced directed migration of HUVECs (Figure 5A), consistent with a role of both NRP1 and NRP2 in endothelial migration. Infection with AdWT NRP1 had little effect on cell migration, whereas the Y297A mutant reduced the number of migrating cells compared with either control or WT adenovirus (Figure 5B). Expression of increasing levels of AdY297A NRP1 caused a greater inhibition of VEGF-A$_{165}$-induced migration, with 90% inhibition at the highest titer selected and, similarly, AdD320A NRP1, which also prevented VEGF-A$_{165}$ binding to NRP1, inhibited VEGF-A$_{165}$–induced migration of HUVECs to a similar extent as Y297A (Figure 5B).

Because NRP1 has also been reported to be important for endothelial cell adhesion, we examined whether non-VEGF-binding NRP1 mutants could affect adhesion of HUVECs to fibronectin. Knockdown of NRP1 using siRNA caused a modest, although statistically significant, decrease in the adhesion of HUVECs to fibronec-
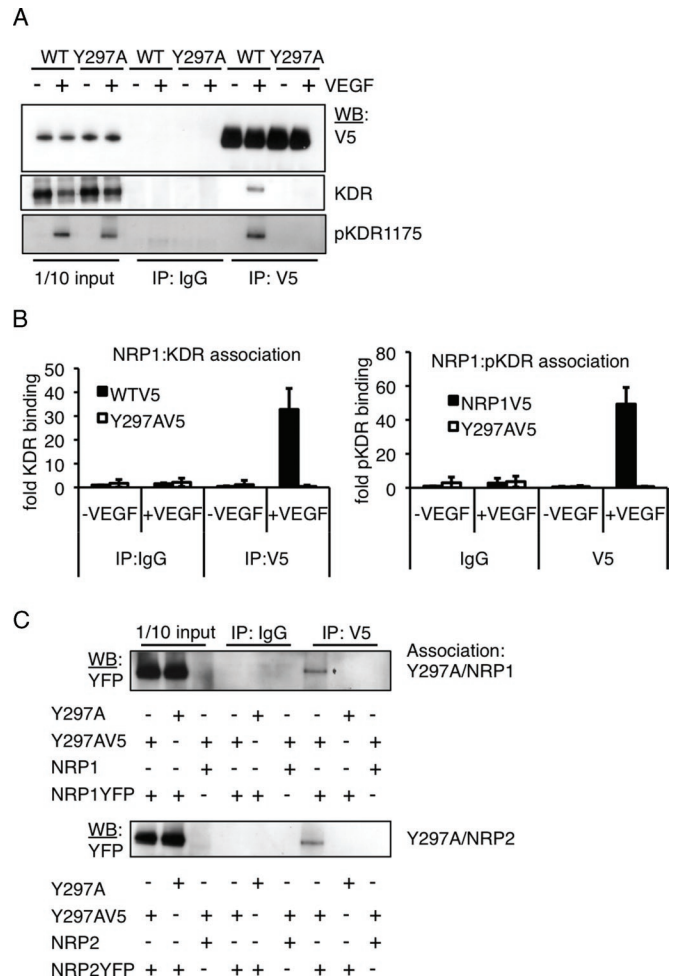
FIGURE 4: VEGF-A$_{165}$ binding to NRP1 is essential for ligand-dependent complex formation between NRP1 and KDR. (A) HUVECs infected with WT NRP1V5 or Y297A NRP1V5 adenoviruses were treated 72 h after infection with VEGF-A$_{165}$ (+) or with vehicle (–) for 10 min, and equal amounts of total cell lysates were used for immunoprecipitation with the indicated antibodies (IP) and detection by Western blotting as indicated (WB). (B) NRP1/KDR (left) and NRP1/pKDR (right) association of five independent experiments was quantified. Data are expressed as means ± SD. (C) COS7 cells were transfected with the plasmid constructs indicated (+) and 48 h later were lysed. Then immunoprecipitations were performed with the antibodies indicated (IP), and immunoprecipitates were immunoblotted as indicated (WB) to determine associations between Y297A NRP1 and either WT NRP1 or WT NRP2.

tin-coated plates consistent with previous findings (unpublished results; Murga *et al.*, 2005). In contrast, adhesion assays performed in the presence or absence of VEGF-A$_{165}$ in HUVECs infected with Ad-LacZ, AdWT NRP1, or AdY297A NRP1 showed no significant differences in the attachment of HUVECs after 48 h (Figure 5C). VEGF-A$_{165}$ treatment also had no significant effect on adhesion.

VEGF-A$_{165}$ binding to NRP1 is required for FAK signaling

An important pathway involved in VEGF-induced migration is phosphorylation of the nonreceptor tyrosine kinase FAK (Abedi and Zachary, 1997; Abu-Ghazaleh *et al.*, 2001). Recent findings suggest that FAK phosphorylation at Y407 plays an important role in VEGF-stimulated signaling leading to endothelial cell migration (Le Boeuf *et al.*, 2006). To address the specific role of VEGF binding to NRP1
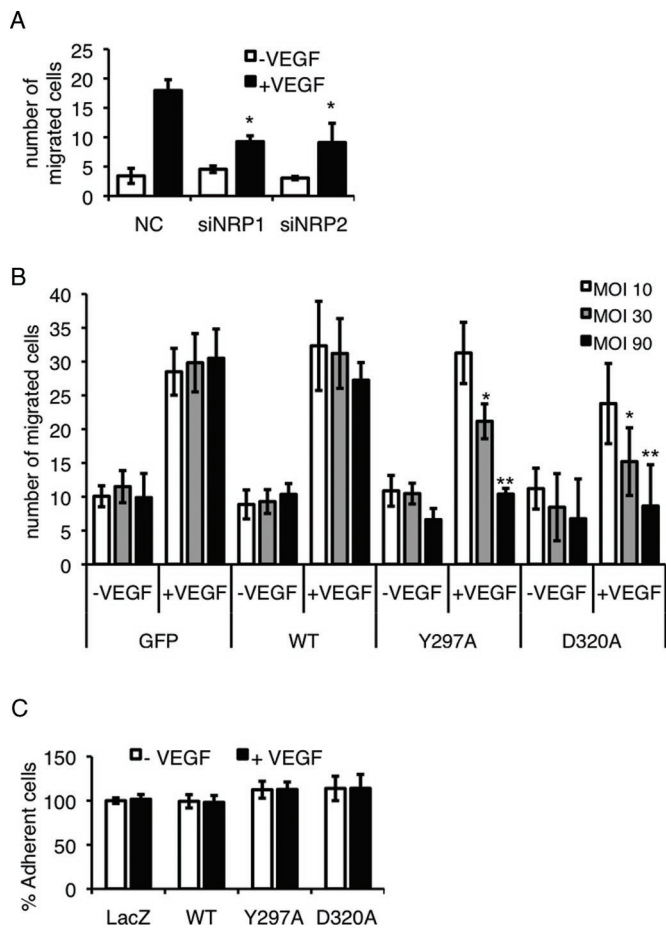
FIGURE 5: VEGF-A$_{165}$ binding to NRP1 is required for migration but not for adhesion. (A) HUVECs were transfected with control siRNA (NC) or siRNA directed against NRP1 or NRP2 as indicated. Cell migration was measured in a transwell assay. Data represent the average number of migrated cells of three independent experiments ± SD; *p < 0.05 vs. NC + VEGF. (B) Migration assay of HUVECs infected with adenoviruses expressing GFP, WT NRP1, Y297A, or D320A NRP1 in transwells at the MOIs indicated. Migrated cells were counted 72 h after infection. Data represent mean numbers of migrated cells ± SD from three independent experiments; *p < 0.05 vs. GFP MOI 30, and **p < 0.01 vs. GFP MOI 90. (C) HUVECs were infected with adenoviruses expressing LacZ, WT NRP1 (WT), Y297A NRP1, or D320A NRP1 as indicated. After 72 h, the attachment of infected cells to fibronectin-covered wells was measured in the presence or absence of 25 ng/ml VEGF-A$_{165}$. Data represent mean fold changes ± SD from three independent experiments.

in this signaling pathway, HUVECs were infected with control GFP, WT NRP1, or Y297A NRP1 adenoviruses, and 72 h after infection quiescent cells were treated with VEGF-A$_{165}$. VEGF-A$_{165}$ stimulation of KDR phosphorylation at Y1175 was similar and not significantly different in HUVECs expressing WT and Y297A NRP1 (Figure 6A). Immunoblotting of lysates from VEGF-treated, infected cells showed that the phosphorylation of Y407 FAK was markedly reduced in cells expressing Y297A NRP1, whereas WT NRP1 had little effect (Figure 6A). Quantification of data from four independent experiments showed that VEGF-A$_{165}$ caused no significant increase in Y407 FAK phosphorylation after a 30-min treatment in Y297A NRP1–expressing cells, whereas VEGF-A$_{165}$ induced Y407 phosphorylation to a similar extent after 10 and 30 min in GFP- and WT NRP1–ex-

pressing cells (Figure 6A). ERK1/2 was activated to a similar extent by VEGF-A$_{165}$ in GFP-, WT-, and Y297A-expressing cells. Our recent findings also indicate that NRP1 knockdown has no significant effect on VEGF-induced ERK1/2 activation (Evans et al., 2011). We also found that knockdown of NRP1 using targeted siRNA caused a marked and significant inhibition of VEGF-A$_{165}$–stimulated KDR1175 phosphorylation, compared with cells transfected with scrambled siRNA. In contrast, NRP2 siRNA caused no significant inhibition of VEGF-A$_{165}$–stimulated KDR1175 phosphorylation (Figure 6B). The phosphorylation of FAK in response to VEGF-A$_{165}$ treatment was also reduced by siRNA-mediated knockdown of NRP1 and NRP2 (Figure 6B).

Effect of non-VEGF-binding NRP1 mutants on angiogenesis

An in vitro tubulogenesis assay was performed to test the effect of NRP1 VEGF-binding mutants on angiogenesis. HUVECs were cultured on a layer of human dermal fibroblasts in the presence or absence of VEGF. Uninfected HUVECs or cells infected with GFP control virus showed an extended network of endothelial cell tubules after 7- to 10-d culture in the presence of VEGF, and cells cultured without VEGF showed little angiogenesis (Figure 7A). Whereas expression of WT NRP1 had no significant effect on the angiogenic response to VEGF, endothelial cells expressing the Y297A NRP1 mutation exhibited a significantly decreased formation of this network of tubules (Figure 7A) as judged by a decrease in both tubule length (Figure 7B) and a reduced number of branchpoints in the tubular network (Figure 7C). Furthermore, a similar inhibitory effect was produced by the nonbinding D320A NRP1 mutant (Figure 7).

DISCUSSION

The purpose of this study was to address the role of VEGF binding to NRP1 in endothelial cells through functional analysis of NRP1 mutants defective in VEGF ligand binding. The b1 domain of NRP1 is essential for VEGF binding (Gu et al., 2002; Mamluk et al., 2002). We have identified Tyr-297 and Asp-320 as two of several residues within the b1 domain of NRP1 which are required for VEGF binding. These residues have recently been shown to be involved in binding of the NRP1 b1 domain in vitro to tuftsin, a natural tetrapeptide with some homology to the C terminus of VEGF-A$_{165}$ (von Wronski et al., 2006; Vander Kooi et al., 2007). Loss of binding in b1 domain mutants is not likely due to major structural changes in the receptor because mutant protein expression and localization to the cell membrane were not affected. We propose that the Y297A and D320A NRP1 mutants, when overexpressed in endothelial cells, act in a dominant-negative manner to inhibit VEGF binding to WT receptors, by forming heterodimers with WT NRP1, which have reduced affinity for VEGF-A$_{165}$. This hypothesis is supported by the finding that differentially tagged forms of Y297A and WT NRPs can be coimmunoprecipitated, indicating that these forms associate spontaneously in dimers or higher-order complexes. This finding suggests that NRP1 homodimerization and NRP1/NRP2 heterodimerization, and/or possibly oligomerization, may play an important role in the formation of high-affinity binding sites for VEGF-A$_{165}$. Several domains in NRP1 may be important for dimerization, including the MAM, transmembrane, and C-terminal domains of NRP1 (Nakamura et al., 1998; Renzi et al., 1999; Roth et al., 2008). Heparin also promotes receptor dimerization and enhanced VEGF-A$_{165}$ binding to NRP1, but failed to rescue VEGF-A$_{165}$ binding to the Y297A mutant NRP1, demonstrating the importance of interaction of the C terminus of VEGF-A$_{165}$ with this residue in the b1 domain (Vander Kooi et al., 2007). The finding that heparin was able to partially restore VEGF-A$_{165}$ binding to other NRP1 b1 domain mutants, which
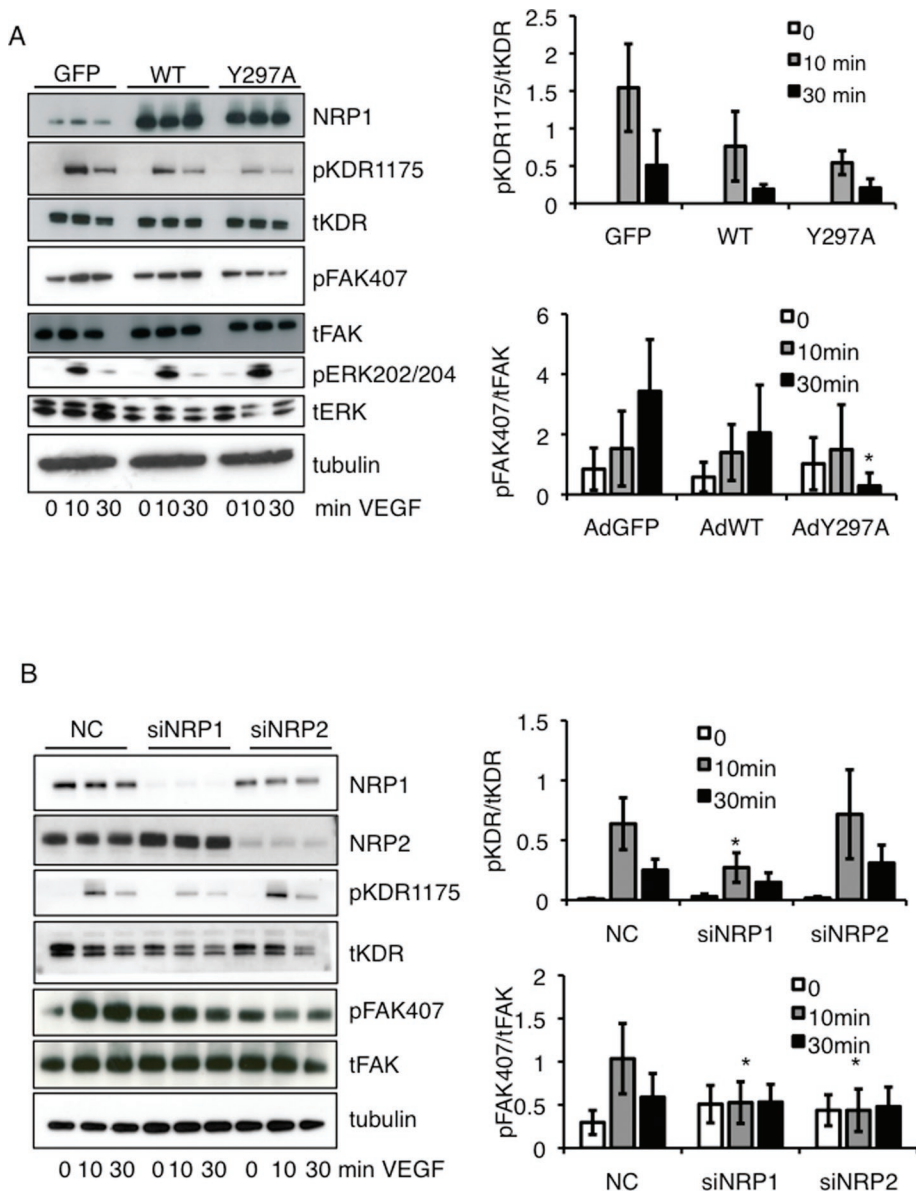
FIGURE 6: VEGF binding to NRP1 is important for FAK Tyr-407 phosphorylation in endothelial cells. (A) HUVECs were infected with GFP, WT NRP1, or Y297A NRP1. Growth medium was replaced by serum-free medium 72 h after infection, and the following day quiescent infected cells were treated with VEGF-A$_{165}$ for the times indicated. Whole-cell extracts were then analyzed by using Western blotting with the indicated antibodies. Blots from panel A (n = 4) were quantified by scanning densitometry to determine the extent of phosphorylation KDR Y1175 and FAK Y407 (right). The bar graph shows the mean ratio of phosphorylated to total protein from four independent experiments ± SD; *p < 0.05 vs. WT 30 min VEGF treatment. (B) HUVECs were transfected with negative control siRNA (NC) or siRNAs targeted to NRP1 or NRP2, and 48 h later were treated with 25 ng/ml VEGF-A$_{165}$ for 10 or 30 min. Cells were then lysed and immunoblotted as indicated. Blots were quantified as described earlier; *p < 0.05 vs. control siRNA.

genesis in a coculture model provides strong evidence that VEGF-A$_{165}$ binding to NRP1 plays an important role in migratory responses important for angiogenesis. Previous work showed that a peptide antagonist that selectively and effectively blocks VEGF binding to NRP1 had no significant effects on VEGF stimulation of proliferation or cell survival (Jia et al., 2006) and that an NRP1 antibody that inhibits VEGF binding to NRP1 only slightly reduced VEGF stimulation of HUVEC proliferation, but caused much greater inhibition of cell migration (Pan et al., 2007). Therefore, previous data do not indicate a major role for VEGF binding to NRP1 in the mitogenic response to VEGF. Although nonbinding NRP1 mutants reduced VEGF-A$_{165}$ binding to HUVECs by up to 45%, the substantial residual binding unaffected by these mutants even at the highest levels of adenovirus used argue strongly that functional dominant-negative effects of Y297A and D320A NRP1 on migration and branching tubulogenesis are not due to a nonspecific effect on binding to other receptors, such as KDR. Interestingly, neither Y297A NRP1 nor VEGF-A$_{165}$ treatment significantly affected endothelial cell adhesion to fibronectin or poly-L-lysine, although NRP1 knockdown did inhibit adhesion. Consistent with this observation, Tyr-297 is not part of an 18-amino-acid stretch in the b1 and b2 domains of NRP1 reported to be sufficient for NRP1-mediated cell adhesion (Shimizu et al., 2000). Previous studies suggest that NRP1-mediated endothelial cell adhesion is independent of VEGF and Sema3A ligands (Murga et al., 2005), and our data now provide direct support for this conclusion.

Inhibition of the VEGF migratory response by Y297A NRP1 may be due, as discussed earlier, to formation of dimers with endogenous WT NRP1, which have reduced affinity for VEGF-A$_{165}$, and as a result either do not participate in complexation with KDR, or form NRP1/KDR complexes with reduced functionality. Previous studies obtained different results for NRP1/KDR complex formation, some demonstrating a strong dependence of NRP1 and KDR association on VEGF-A treatment (Soker et al., 2002; Pan et al., 2007), whereas others found that complex formation was a largely constitutive process, occurring in the absence of VEGF-A (Whittaker et al., 2001; Shraga-Heled et al., 2007). The differences between these studies may reflect technical factors relating to the conditions and reagents used for immunoprecipitation, as well as choice of endothelial cell type, and heterogeneities among different cell preparations. We found that NRP1 complex formation with KDR was strongly induced by treatment with VEGF-A$_{165}$. We do not preclude, however, that constitutive formation of NRP1/KDR complexes may be biologically

caused substantial loss of binding in the absence of heparin suggests, however, that heparin is able to mediate binding interactions between the VEGF-A$_{165}$ C terminus and the b1 domain. Although Sema3A binding to NRP1 also requires the b1 domain, the Y297A mutation does not affect the binding of Sema3A, and this allowed us to address the specific role of VEGF-A$_{165}$ binding to NRP1.

The finding that expression of the Y297A and D320A NRP1 mutants reduced high-affinity VEGF-A$_{165}$ binding to endothelial cells and VEGF-A$_{165}$ stimulation of endothelial cell migration and tubulo-
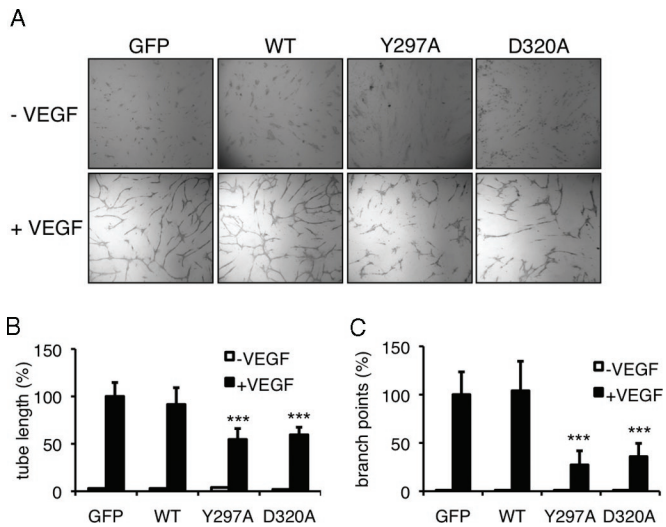
FIGURE 7: VEGF binding to NRP1 is important for angiogenesis in a coculture assay. (A) Human dermal fibroblasts were grown in a 24-well format to confluence. HUVECs were infected with adenoviruses encoding GFP, WT NRP1, Y297A NRP1, or D320A NRP1, and 72 h after infection were seeded (10,000 cells per well) on top of the fibroblast cell layer. Cell cocultures were then maintained for 7 d in the presence of 0.5% serum alone (-VEGF) or 0.5% serum plus 25 ng/ml VEGF-A_{165} (+VEGF). Endothelial cells were then visualized by immunostaining for vWF. (B and C) Quantitation of coculture assays in (A). The bar graph shows the mean ± SD total tubule length (B) or number of branchpoints (C) counted in three independent experiments; ***p < 0.001 vs. GFP + VEGF.

important, and although the mechanisms underlying this phenomenon are currently unclear, one possibility is that endogenous VEGF-A_{165} production may mediate basal association between NRP1 and KDR acting in either an autocrine or intracrine manner. Our data further showed that expression of the Y297A NRP1 mutant prevented VEGF-A_{165}–induced complex formation between NRP1 and KDR, indicating that VEGF-A_{165} binding to NRP1 is essential for formation of NRP1/KDR heterodimers either alone or as homodimers or oligomers with WT NRP1, and that these heterocomplexes may be rapidly destabilized by subsequent VEGF-A_{165} binding to KDR. We previously reported that siRNA-mediated knockdown of NRP1 in HUVECs reduced KDR expression both under basal unstimulated conditions or after VEGF-A_{165} stimulation (Holmes and Zachary, 2008). Thus it is plausible that, in the presence of an NRP1 mutant unable to bind VEGF-A, NRP1/KDR heterocomplexes may be rapidly destabilized by subsequent VEGF-A_{165} binding to KDR in part because of increased KDR lability. This possibility warrants further investigation.

Generation of the Y297A NRP1 VEGF-A_{165} binding mutant also provided a tool with which we were able to dissect the contribution of NRP1 to VEGF-A_{165} endothelial cell signaling. The KDR-HSP90-FAKpTyr407 pathway is critical for the assembly of focal adhesions and endothelial cell migration (Rousseau et al., 2000; Le Boeuf et al., 2004). VEGF stimulates the tyrosine phosphorylation of FAK and its major substrate, paxillin (Abedi and Zachary, 1997). Several phosphorylation sites in FAK mediate signaling from receptor tyrosine kinases and integrins to promote cell migration and blood vessel morphogenesis in vivo (Sieg et al., 2000; Ilic et al., 2003), and Tyr-407 phosphorylation plays a critical role in mediating the response to VEGF (Le Boeuf et al., 2006). Both VEGF and hepatocyte growth factor (HGF) activate FAK in endothelial cells with different kinetics, however, and FAK is recruited to different subsets of focal adhesions

in response to these cytokines (Sulpice et al., 2009). Because HGF can also bind to NRP1 (Sulpice et al., 2008) it will be interesting to investigate in future work the effect of the Y297A NRP1 mutant on HGF signaling. Our finding that Y297A NRP1 reduces FAK phosphorylation at Tyr-407 suggests that VEGF-A_{165} binding to NRP1 plays a key role in focal adhesion signaling important for cell migration. It is noteworthy that Y297A NRP1 expression had no significant effect on VEGF-A_{165}–induced activation of KDR or ERK1/2 compared with WT NRP1. The lack of effect of Y297A NRP1 on KDR phosphorylation probably reflects the fact that KDR activation by VEGF-A_{165} is mainly independent of NRP1. This conclusion is consistent with the finding that NRP1-directed antibody, which selectively blocks VEGF-A_{165} binding to NRP1 and inhibits VEGF-A_{165}–induced endothelial cell migration, had little effect on KDR or ERK activation in HUVECs (Pan et al., 2007). Taken together, these findings indicate that NRP1 plays a role in specific KDR signaling pathways such as FAK Y407, but is dispensable for KDR activation and signaling pathways mediated via KDR phosphorylation at Y1175 such as ERK activation.

We also identified an important role for NRP2 in mediating VEGF-induced migration in HUVECs, based on the inhibitory effects of NRP2 knockdown. ^{125}I-VEGF-A_{165} exhibited specific binding to cells expressing NRP2, but bound to NRP2 with significantly lower affinity than to NRP1. These data are consistent with a recent study reporting a dissociation constant (K_d) of 5.2 nM for NRP2, compared with the K_d for VEGF-A_{165} binding to NRP1 of 0.2–0.3 nM (Soker et al., 1998; Geretti et al., 2007). The finding that overexpression of Y297A NRP1 was able to reduce ^{125}I-VEGF-A_{165} binding to NRP2 and strongly inhibit VEGF-induced cell migration indicates that this mutant also exerts a dominant-negative effect on the NRP2-dependent migratory response of endothelial cells. Because Y297A NRP1 was able to associate with NRP2, this effect is likely to be due to the formation of Y297A NRP1/NRP2 heterodimers with a reduced capacity to bind VEGF and to participate in functional complexes of NRP2 with other receptors. Given that weak binding of VEGF-A_{165} appears to occur at concentrations of VEGF-A_{165} required for biological effects in endothelial cells such as migration or angiogenesis, such as were used in this study, the biological relevance of VEGF-A_{165} binding to NRP2 in cells is unclear. Thus it is plausible that the major mechanism through which NRP2 contributes to VEGF-A_{165}–dependent migration in human endothelial cells is through heterodimerization with NRP1 rather than direct binding of VEGF-A_{165} to NRP2.

In this article, we have identified residues essential for VEGF-A_{165} binding to NRP1, which constitute part of the putative binding pocket for VEGF-A_{165} in the NRP1 b1 domain, defined by computational analysis of the b1 domain structure, and inferred from the crystal structure of the b1 domain. Functional analysis of two binding deficient NRP1 mutants revealed an unexpected dominant negative effect of these mutants on VEGF-A_{165} binding to WT NRP1 and on VEGF-A_{165} stimulation of migration and signaling mediating cell migration. These findings provide strong evidence for the importance of VEGF-A_{165} binding to NRP1 in endothelial cell migration, and also highlight the role of NRP1 in linking the VEGF-A_{165}/KDR axis to specific chemotactic signaling pathways. Identification of key residues in the VEGF-A_{165} binding pocket of NRP1 will also be helpful in the future rational design of small molecule inhibitors of ligand binding to NRP1.

MATERIALS AND METHODS
Molecular modeling
Possible binding sites in the NRP1 b1 domain were searched using the SYBYL SITEID module (SYBYL 7.0; Tripos, St. Louis, MO).

Materials

Recombinant VEGF-A$_{165}$ was obtained from Invitrogen (Carlsbad, CA). Heparin was purchased from Sigma (St. Louis, MO). Antibodies purchased from Santa Cruz Biotechnology (Santa Cruz, CA) were NRP1 (sc-7239), NRP2 (sc-13117), KDR (sc-504), GAPDH (sc-20357), and α-tubulin (sc-8035). Phospho-FAK407 (44650G) and GFP (A6455) were obtained from Invitrogen; phospho-KDR (#2478), FAK (#3285), phospho-ERK (#9101) were obtained from Cell Signaling Technology (Danvers, MA); KDR (#101-M32) from ReliaTech (Wolfenbüttel, Germany); vWF (ab6994) from Abcam (Cambridge, UK); and anti-V5 agarose (A7345) from Sigma.

Plasmids and adenoviral constructs

The open reading frames of human NRP1 and NRP2 were cloned into pENTR/D-TOPO by directional TOPO-cloning (Invitrogen, Paisley, UK). Subsequently, plasmid expression constructs (pcDNA3.2/V5-DEST) and adenoviral vectors encoding NRP1 constructs (pAd/CMV/V5-DEST) were generated by recombination using the gateway system (Invitrogen). Mutagenesis of human NRP1 in pENTR was performed using the QuickChange kit (Stratagene, La Jolla, CA). All constructs were confirmed by DNA sequencing. YFP-tagged NRP1 WT, Y297A NRP1, and NRP2 were generated using the pcDNA6.2/YFP-GW/TOPO vector (Invitrogen).

Cell culture and transfection

HUVECs were purchased from Lonza (Basel, Switzerland) and cultured in complete endothelial cell basal medium (Lonza) supplemented with 10% fetal bovine serum (FBS). The day before treatment of HUVECs the culture medium was replaced by serum-free medium. COS7 cells were obtained from the ECACC (European Collection of Cell Cultures) and maintained in DMEM supplemented with 10% FBS (Invitrogen). Cells were transfected with Lipofectamine 2000 (Invitrogen), according to the manufacturer's instructions.

Western blotting

After treatment, cells were washed in ice-cold phosphate-buffered saline (PBS) and lysed in radio-immunoprecipitation assay (RIPA) buffer (NEB, Hitchin, UK) with 0.5 µl/ml Protease Inhibitor Cocktail (Sigma, Poole, UK) and 1 mM phenylmethylsulfonyl fluoride. Proteins were separated on NuPage 4–12% Bis-Tris gels using 3-(N-morpholino)-propanesulfonic acid running buffer systems and transferred to Invitrolon polyvinylidene fluoride membranes (Invitrogen). Membranes were blocked in 5% nonfat dried milk in PBS and 0.1% Tween 20 and incubated with primary antibodies overnight at 4°C. Immunoreactive bands were detected by horseradish peroxidase (HRP)-conjugated secondary antibodies and chemiluminescent detection (ECL Plus; GE Healthcare, Little Chalfont, UK).

Immunofluorescence staining

Cells were fixed in 4% formaldehyde in PBS followed by permeabilization in 0.02% Triton X-100 in PBS. Fixed cells were incubated with anti-NRP1 (Santa Cruz) or Alexa Fluor phalloidin (Invitrogen) overnight at 4°C in 1% bovine serum albumin (BSA), 0.1% Tween 20 in PBS. Confocal imaging was performed using a Bio-Rad (Hercules, CA) Radiance 2100 laser and upright Nikon Eclipse E1000 microscope.

Flow cytometry

Confluent COS7 cells were harvested with dissociation buffer (C1914; Sigma) and washed with PBS/1% BSA/20 mM HEPES. Cells were incubated with anti-NRP1 antibody (CD304-PE; Miltenyi Biotec, Bisley, UK) for 20 min at 4°C. Cells were washed in PBS/1% BSA/20 mM HEPES. Data were analyzed with the FACSCalibur system (BD Biosciences, Franklin Lakes, NJ).

Immunoprecipitations

Coimmunoprecipitations involving NRP1, KDR, and V5-tagged and YFP-tagged NRP1 and NRP2 constructs were performed essentially as described (Prahst *et al.*, 2008). Briefly, whole-cell extracts from HUVECs were prepared in lysis buffer and incubated with 1 µg of antibody and 30 µl of Sepharose G beads overnight at 4°C with rotation. Precipitated protein complexes were washed three times in ice-cold PBS containing protease and phosphatase inhibitors and eluted in 2× LDS buffer (Invitrogen) at 70°C for 10 min.

Tubulogenesis assay

In vitro angiogenesis was determined by using a coculture tubulogenesis assay (Friis *et al.*, 2003). Briefly, human dermal fibroblasts were grown to confluence in 24-well plates in M106 medium supplemented with low serum growth supplement (Invitrogen). Medium was replaced, and 10,000 HUVECs were plated on top of the fibroblast layer cultured in complete endothelial growth medium supplemented with 1% FBS. HUVECs and fibroblasts were propagated in coculture for 7 d at 37°C and 5% CO$_2$. Cells in coculture were fixed in absolute ethanol for 2 h at room temperature, and HUVECs were identified by incubating with anti–von Willebrand factor antibody in PBS-Tween 20 with 5% BSA overnight at 4°C. Bound antibody was detected with biotinylated secondary antibody (Chemicon, Temecula, CA) and ABC (Vector Laboratories, Burlingame, CA) with diaminobenzidine staining (Sigma). Photomicrographs of von Willebrand factor–stained cocultures were analyzed using ImageJ software. The length of all tubular structures (stained endothelial cells) and the number of branching points were measured in four representative microscopic fields per well.

Cell migration assay

Migration of HUVECs was measured as described previously using Transwell membranes (BD Biosciences; Evans *et al.*, 2008).

Cell adhesion assay

Cell adhesion was measured using the InnoCyte ECM Cell Adhesion Assay with fibronectin-covered plates (Calbiochem, San Diego, CA).

VEGF-A$_{165}$ and Sema3A binding assay

After transfection with NRP1 constructs, COS7 cells were washed in ice-cold PBS and incubated with 2 nM bt-rhVEGF-A$_{165}$ (R&D Systems, Minneapolis, MN) in DMEM with 0.1% BSA for 2 h at 4°C with agitation. After incubation, cells were washed three times in ice-cold PBS and incubated with streptavidin-HRP (R&D Systems) in PBS with 1% BSA for 30 min at room temperature with agitation. Cells were then washed three times in PBS before detection with substrate reagent (R&D Systems) for 15 min. The reaction was stopped with stopping solutions, and signal intensity was quantified using a Tecan Genios plate reader at A450 nm with a reference wavelength of 595 nm. A Sema3A binding assay was performed as described (Narazaki and Tosato, 2006). Briefly, cells were blocked with PBS-Tween 20 with 5% dry milk and then incubated with 1 µg/ml Sema3A/Fc (R&D Systems) for 2 h at 4°C with agitation. The antibody solution was removed, and cells were washed three times with PBS-Tween 20. Bound Sema3A was detected with anti- IgG/Fc-HRP antibody (Autogen Bioclear, Calne, Wiltshire, UK).

^{125}I-VEGF-A$_{165}$ (~50 μCi/μg; Lofstrand Labs, Gaithersburg, MD) binding was performed essentially as described (Jia *et al.*, 2006). Confluent cells in 24-well plates were washed twice with PBS. At 4°C the indicated concentrations of ^{125}I-VEGF-A$_{165}$ with or without 100-fold excess of unlabeled VEGF-A$_{165}$ (R&D Systems) diluted in binding medium (Iscove's modified Dulbecco's medium [IMEM] containing 0.1% BSA) were added. After 2 h of incubation at 4°C, the medium was aspirated and washed three times with cold PBS. The cells were lysed with 0.25 M NaOH, 0.5% SDS solution, and the bound radioactivity of the lysates was measured in a γ counter. Specific binding was determined as the total binding obtained in the absence of unlabeled VEGF-A$_{165}$ minus the nonspecific binding in the presence of 100-fold excess unlabeled VEGF-A$_{165}$ (R & D Systems).

Statistical methods

Results are presented as mean ± SD. The statistical significance of differences between samples was determined by a two-tailed Student's *t* test.

REFERENCES

Abedi H, Zachary I (1997). Vascular endothelial growth factor stimulates tyrosine phosphorylation and recruitment to new focal adhesions of focal adhesion kinase and paxillin in endothelial cells. J Biol Chem 272, 15442–15451.

Abu-Ghazaleh R, Kabir J, Jia H, Lobo M, Zachary I (2001). Src mediates stimulation by vascular endothelial growth factor of the phosphorylation of focal adhesion kinase at tyrosine 861, and migration and anti-apoptosis in endothelial cells. Biochem J 360, 255–264.

Cai H, Reed RR (1999). Cloning and characterization of neuropilin-1-interacting protein: a PSD-95/Dlg/ZO-1 domain-containing protein that interacts with the cytoplasmic domain of neuropilin-1. J Neurosci 19, 6519–6527.

Chittenden TW et al. (2006). Selective regulation of arterial branching morphogenesis by synectin. Dev Cell 10, 783–795.

Evans IM, Britton G, Zachary IC (2008). Vascular endothelial growth factor induces heat shock protein (HSP) 27 serine 82 phosphorylation and endothelial tubulogenesis via protein kinase D and independent of p38 kinase. Cell Signal 20, 1375–1384.

Evans IM, Yamaji M, Britton G, Pellet-Many C, Lockie C, Zachary IC, Frankel P (2011). Neuropilin-1 signalling through p130Cas tyrosine phosphorylation is essential for growth factor dependent migration of glioma and endothelial cells. Mol Cell Biol 31, 1174–1185.

Friis T, Kjaer Sorensen B, Engel AM, Rygaard J, Houen G (2003). A quantitative ELISA-based co-culture angiogenesis and cell proliferation assay. Acta Pathol Microbiol Scand C Immunol 111, 658–668.

Fujisawa H, Kitsukawa T (1998). Receptors for collapsin/semaphorins. Curr Opin Neurobiol 8, 587–592.

Gao Y, Li M, Chen W, Simons M (2000). Synectin, syndecan-4 cytoplasmic domain binding PDZ protein, inhibits cell migration. J Cell Physiol 184, 373–379.

Gerber HP, McMurtrey A, Kowalski J, Yan M, Keyt BA, Dixit V, Ferrara N (1998). Vascular endothelial growth factor regulates endothelial cell survival through the phosphatidylinositol 3′-kinase/Akt signal transduction pathway. Requirement for Flk-1/KDR activation. J Biol Chem 273, 30336–30343.

Geretti E, Shimizu A, Kurschat P, Klagsbrun M (2007). Site-directed mutagenesis in the B-neuropilin-2 domain selectively enhances its affinity to VEGF$_{165}$, but not to semaphorin 3F. J Biol Chem 282, 25698–25707.

Gille H, Kowalski J, Li B, LeCouter J, Moffat B, Zioncheck TF, Pelletier N, Ferrara N (2001). Analysis of biological effects and signaling properties of Flt-1 (VEGFR-1) and KDR (VEGFR-2). A reassessment using novel receptor-specific vascular endothelial growth factor mutants. J Biol Chem 276, 3222–3230.

Gliki G, Abu-Ghazaleh R, Jezequel S, Wheeler-Jones C, Zachary I (2001). Vascular endothelial growth factor-induced prostacyclin production is mediated by a protein kinase C (PKC)-dependent activation of extracellular signal-regulated protein kinases 1 and 2 involving PKC-delta and by mobilization of intracellular Ca2+. Biochem J 353, 503–512.

Gu C, Limberg BJ, Whitaker GB, Perman B, Leahy DJ, Rosenbaum JS, Ginty DD, Kolodkin AL (2002). Characterization of neuropilin-1 structural features that confer binding to semaphorin 3A and vascular endothelial growth factor 165. J Biol Chem 277, 18069–18076.

He Z, Tessier-Lavigne M (1997). Neuropilin is a receptor for the axonal chemorepellent Semaphorin III. Cell 90, 739–751.

Holmes DI, Zachary I (2005). The vascular endothelial growth factor (VEGF) family: angiogenic factors in health and disease. Genome Biol 6, 209.

Holmes DI, Zachary IC (2008). Vascular endothelial growth factor regulates stanniocalcin-1 expression via neuropilin-1-dependent regulation of KDR and synergism with fibroblast growth factor-2. Cell Signal 20, 569–579.

Ilic D, Kovacic B, McDonagh S, Jin F, Baumbusch C, Gardner DG, Damsky CH (2003). Focal adhesion kinase is required for blood vessel morphogenesis. Circ Res 92, 300–307.

Jarvis A et al. (2010). Small molecule inhibitors of the neuropilin-1 vascular endothelial growth factor A (VEGF-A) interaction. J Med Chem 53, 2215–2226.

Jia H et al. (2006). Characterisation of a bicyclic peptide neuropilin-1 (NP-1) antagonist (EG3287) reveals importance of vascular endothelial growth factor exon 8 for NP-1 binding and role of NP-1 in KDR signalling. J Biol Chem 281, 13493–13502.

Kawasaki T, Kitsukawa T, Bekku Y, Matsuda Y, Sanbo M, Yagi T, Fujisawa H (1999). A requirement for neuropilin-1 in embryonic vessel formation. Development 126, 4895–4902.

Kitsukawa T, Shimizu M, Sanbo M, Hirata T, Taniguchi M, Bekku Y, Yagi T, Fujisawa H (1997). Neuropilin-semaphorin III/D-mediated chemorepulsive signals play a crucial role in peripheral nerve projection in mice. Neuron 19, 995–1005.

Kolodkin AL, Levengood DV, Rowe EG, Tai YT, Giger RJ, Ginty DD (1997). Neuropilin is a semaphorin III receptor. Cell 90, 753–762.

Le Boeuf F, Houle F, Huot J (2004). Regulation of vascular endothelial growth factor receptor 2-mediated phosphorylation of focal adhesion kinase by heat shock protein 90 and Src kinase activities. J Biol Chem 279, 39175–39185.

Le Boeuf F, Houle F, Sussman M, Huot J (2006). Phosphorylation of focal adhesion kinase (FAK) on Ser732 is induced by rho-dependent kinase and is essential for proline-rich tyrosine kinase-2-mediated phosphorylation of FAK on Tyr407 in response to vascular endothelial growth factor. Mol Biol Cell 17, 3508–3520.

Lee CC, Kreusch A, McMullan D, Ng K, Spraggon G (2003). Crystal structure of the human neuropilin-1 b1 domain. Structure 11, 99–108.

Mamluk R, Gechtman Z, Kutcher ME, Gasiunas N, Gallagher J, Klagsbrun M (2002). Neuropilin-1 binds vascular endothelial growth factor 165, placenta growth factor-2, and heparin via its b1b2 domain. J Biol Chem 277, 24818–24825.

Murga M, Fernandez-Capetillo O, Tosato G (2005). Neuropilin-1 regulates attachment in human endothelial cells independently of vascular endothelial growth factor receptor-2. Blood 105, 1992–1999.

Nakamura F, Tanaka M, Takahashi T, Kalb RG, Strittmatter SM (1998). Neuropilin-1 extracellular domains mediate semaphorin D/III-induced growth cone collapse. Neuron 21, 1093–1100.

Narazaki M, Tosato G (2006). Ligand-induced internalization selects use of common receptor neuropilin-1 by VEGF165 and semaphorin3A. Blood 107, 3892–3901.

Pan Q et al. (2007). Blocking neuropilin-1 function has an additive effect with anti-VEGF to inhibit tumor growth. Cancer Cell 11, 53–67.

Pellet-Many C, Frankel P, Jia H, Zachary IC (2008). Neuropilins: structure, function and role in disease. Biochem J 411, 211–226.

Prahst C, Heroult M, Lanahan AA, Uziel N, Kessler O, Shraga-Heled N, Simons M, Neufeld G, Augustin HG (2008). Neuropilin-1-VEGFR-2 complexing requires the PDZ-binding domain of neuropilin-1. J Biol Chem 283, 25110–25114.

Renzi MJ, Feiner L, Koppel AM, Raper JA (1999). A dominant negative receptor for specific secreted semaphorins is generated by deleting an extracellular domain from neuropilin-1. J Neurosci 19, 7870–7880.

Rossignol M, Gagnon ML, Klagsbrun M (2000). Genomic organization of human neuropilin-1 and neuropilin-2 genes: identification and distribution of splice variants and soluble isoforms. Genomics 70, 211–222.

Roth L, Nasarre C, Dirrig-Grosch S, Aunis D, Cremel G, Hubert P, Bagnard D (2008). Transmembrane domain interactions control biological functions of neuropilin-1. Mol Biol Cell 19, 646–654.

Rousseau S, Houle F, Kotanides H, Witte L, Waltenberger J, Landry J, Huot J (2000). Vascular endothelial growth factor (VEGF)-driven actin-based motility is mediated by VEGFR2 and requires concerted activation of stress-activated protein kinase 2 (SAPK2/p38) and geldanamycin-sensitive phosphorylation of focal adhesion kinase. J Biol Chem 275, 10661–10672.

Shimizu M, Murakami Y, Suto F, Fujisawa H (2000). Determination of cell adhesion sites of neuropilin-1. J Cell Biol 148, 1283–1293.

Shraga-Heled N, Kessler O, Prahst C, Kroll J, Augustin H, Neufeld G (2007). Neuropilin-1 and neuropilin-2 enhance VEGF121 stimulated signal transduction by the VEGFR-2 receptor. FASEB J 21, 915–926.

Sieg DJ, Hauck CR, Ilic D, Klingbeil CK, Schaefer E, Damsky CH, Schlaepfer DD (2000). FAK integrates growth-factor and integrin signals to promote cell migration. Nat Cell Biol 2, 249–256.

Soker S, Miao HQ, Nomi M, Takashima S, Klagsbrun M (2002). VEGF165 mediates formation of complexes containing VEGFR-2 and neuropilin-1 that enhance VEGF165-receptor binding. J Cell Biochem 85, 357–368.

Soker S, Takashima S, Miao HQ, Neufeld G, Klagsbrun M (1998). Neuropilin-1 is expressed by endothelial and tumor cells as an isoform-specific receptor for vascular endothelial growth factor. Cell 92, 735–745.

Sulpice E, Ding S, Muscatelli-Groux B, Berge M, Han ZC, Plouet J, Tobelem G, Merkulova-Rainon T (2009). Cross-talk between the VEGF-A and HGF signalling pathways in endothelial cells. Biol Cell 101, 525–539.

Sulpice E, Plouet J, Berge M, Allanic D, Tobelem G, Merkulova-Rainon T (2008). Neuropilin-1 and neuropilin-2 act as coreceptors, potentiating proangiogenic activity. Blood 111, 2036–2045.

Takahashi T, Yamaguchi S, Chida K, Shibuya M (2001). A single autophosphorylation site on KDR/Flk-1 is essential for VEGF-A-dependent activation of PLC-gamma and DNA synthesis in vascular endothelial cells. EMBO J 20, 2768–2778.

Thakker GD, Hajjar DP, Muller WA, Rosengart TK (1999). The role of phosphatidylinositol 3-kinase in vascular endothelial growth factor signaling. J Biol Chem 274, 10002–10007.

Vander Kooi CW, Jusino MA, Perman B, Neau DB, Bellamy HD, Leahy DJ (2007). Structural basis for ligand and heparin binding to neuropilin B domains. Proc Natl Acad Sci USA 104, 6152–6157.

von Wronski MA et al. (2006). Tuftsin binds neuropilin-1 through a sequence similar to that encoded by exon 8 of vascular endothelial growth factor. J Biol Chem 281, 5702–5710.

Wang L, Mukhopadhyay D, Xu X (2006). C terminus of RGS-GAIP-interacting protein conveys neuropilin-1-mediated signaling during angiogenesis. FASEB J 20, 1513–1515.

Wang L, Zeng H, Wang P, Soker S, Mukhopadhyay D (2003). Neuropilin-1-mediated vascular permeability factor/vascular endothelial growth factor-dependent endothelial cell migration. J Biol Chem 278, 48848–48860.

Whitaker GB, Limberg BJ, Rosenbaum JS (2001). Vascular endothelial growth factor receptor-2 and neuropilin-1 form a receptor complex that is responsible for the differential signaling potency of VEGF$_{165}$ and VEGF$_{121}$. J Biol Chem 276, 25520–25531.